Brain developmental trajectories associated with childhood stuttering persistence and recovery

Ho Ming Chow [a], Emily O. Garnett [b,1], Simone P.C. Koenraads [c,1], Soo-Eun Chang [b,*]

[a] *University of Delaware, Department of Communication Sciences and Disorders, Newark, DE 19713, USA*
[b] *Department of Psychiatry, Michigan Medicine, University of Michigan, Ann Arbor, MI 48109, USA*
[c] *Erasmus University Medical Center, 1315 GD Rotterdam, the Netherlands*

ARTICLE INFO

ABSTRACT

Stuttering is a neurodevelopmental disorder affecting 5–8 % of preschool-age children, continuing into adulthood in 1 % of the population. The neural mechanisms underlying persistence and recovery from stuttering remain unclear and little information exists on neurodevelopmental anomalies in children who stutter (CWS) during preschool age, when stuttering symptoms typically first emerge. Here we present findings from the largest longitudinal study of childhood stuttering to date, comparing children with persistent stuttering (pCWS) and those who later recovered from stuttering (rCWS) with age-matched fluent peers, to examine the developmental trajectories of both gray matter volume (GMV) and white matter volume (WMV) using voxel-based morphometry. A total of 470 MRI scans were analyzed from 95 CWS (72 pCWS and 23 rCWS) and 95 fluent peers between 3 and 12 years of age. We examined overall group and group by age interactions in GMV and WMV in preschool age (3–5 years old) and school age (6–12 years old) CWS and controls, controlling for sex, IQ, intracranial volume, and socioeconomic status. The results provide broad support for a possible basal ganglia-thalamocortical (BGTC) network deficit starting in the earliest phases of the disorder and point to normalization or compensation of earlier occurring structural changes associated with stuttering recovery.

1. Introduction

Developmental stuttering is a complex neurodevelopmental disorder (Smith and Weber, 2017) that disrupts the fluent flow of speech production. It is characterized by frequently occurring involuntary repetitions and prolongations in speech sounds, in addition to prolonged articulatory posture, and/or avoidance and struggle behaviors (Van Riper, 1971). Stuttering affects 5–8 % of preschool-age children (Yairi and Ambrose, 2013) and remains as a chronic speech disorder in 1 % of the general population. Typical onset of stuttering is reported to occur at 30–48 months (Bloodstein and Ratner, 2008; Reilly et al., 2013; Yairi and Ambrose, 2005) with approximately 80 % of children naturally recovering 24–36 months after the onset of stuttering (Yairi and

Ambrose, 2013, 2005, 1999). Around this same developmental period, the neural systems supporting executive function, language, and speech-motor control undergo rapid and vigorous development (Smith and Weber, 2017; Almli et al., 2007; Chang et al., 2019; Friederici, 2006; Gilmore et al., 2018).

In the past 20 years, an increasing number of neuroimaging studies have been conducted to understand the possible neural bases of stuttering. Convergent findings from systematic reviews and meta-analyses have highlighted several neuroanatomical differences in children and adults who stutter (AWS) compared to fluent speakers (Smith and Weber, 2017; Chang et al., 2019; Belyk et al., 2015; Budde, 2014; Ingham et al., 2005; Neef et al., 2015). Structural and functional anomalies in the left speech motor neural system, including the inferior frontal

gyrus (IFG), posterior superior temporal gyrus (STG), basal ganglia-thalamo-cortical (BGTC) loop and the cerebellum have been associated with stuttering (see Chang et al., 2019 for review). In addition to gray matter anomalies, children who stutter (CWS) were found to have less white matter volume (WMV) bilaterally in the forceps minor of the corpus callosum (Beal et al., 2013) while another study found no significant differences (Choo et al., 2012). Several diffusion tensor imaging (DTI) studies have repeatedly reported that the anisotropic diffusivity in the corpus callosum and the left superior longitudinal / arcuate fasciculi (SLF / AF) is lower in children and AWS than controls who do not stutter (Neef et al., 2015; Chow and Chang, 2017) suggesting that sensorimotor integration and inter-hemispheric connections may be affected in stuttering. Putting these results in the context of a recent theoretical perspective (Guenther, 2016), three distinct but not mutually exclusive loci of impaired neural processing along the BGTC network was proposed to occur to lead to stuttering, reviewed in Chang and Guenther (Chang and Guenther, 2020): first is the impairment in the BG proper (PDS-1); second, impairment of axonal projections between cortex, BG, and thalamus (PDS-2); and impairment in cortical processing among cortical areas supporting cognitive processing, sensory areas, and motor regions including the primary motor, premotor, and supplementary motor areas (PDS-3).

Many of these past studies, however, only examined AWS with small sample sizes (e.g., N < 12 per group), limiting the ability to characterize neurodevelopmental differences associated with stuttering persistence and recovery in children who stutter. Moreover, to date few studies have investigated neuroanatomical differences in children at or near the onset of stuttering (before 6 years of age). Examining children close to symptom onset is necessary to better understand the neural mechanisms that lead to the emergence of developmental stuttering (Packman et al., 2022). That is, neuroanatomical differences that are present near stuttering onset could help clarify what differences may be attributed to trait-linked differences associated with the disorder, compared to later occurring, adaptive changes that are more likely to be present in those who have been stuttering for many years. Furthermore, because stuttering becomes a chronic condition or resolves itself within a few years of onset in most CWS, it is important to examine the *developmental trajectories* of the brain during this critical period.

Children who go on to develop chronic, persistent stuttering may be those with neuroanatomical differences relative to their non-stuttering peers at stuttering onset that are not resolved as they become older and continue to stutter. Maladaptive changes may occur in additional brain areas as stuttering becomes chronic. In children who recover from stuttering (rCWS), on the other hand, normalization and/or successful compensations for prior deficits associated with stuttering onset may occur. In Chow and Chang (Chow and Chang, 2017) for example, anisotropic diffusion measures that reflect white matter coherence pointed to decreased structural connectivity in several major tracts including the left AF and the corpus callosum in CWS regardless of eventual persistence or recovery. What differentiated the recovered and persistent groups, however, was that the recovered group exhibited age-related increases in these tracts (e.g., the corpus collosum), while the persistent group showed plateaued, or even decreasing white matter integrity with age. The Chow and Chang (Chow and Chang, 2017) study is the only longitudinal study to date that examined neuroanatomical differences occurring across development in persistent and recovered groups of CWS. This study was limited to examining white matter; thus, it is currently unknown what gray matter anomalies may be present near symptom onset, and further, whether age related gray matter changes differentiate children who persist versus recover from stuttering. Results from previous studies have pointed to deficiencies involving the BGTC loop, including function of the basal ganglia proper, cortical-subcortical connectivity, and cortico-cortical connectivity including auditory-motor regions (Chang and Guenther, 2020). It is unclear at this time whether these deficits occur near onset of the disorder, and whether recovery of stuttering is associated with normalization of the deficits in the BGTC

loop, or perhaps compensations by other structures such as the cerebellum, an area that has been theorized to play a compensatory role in response to possible core deficits in the basal ganglia (Alm, 2004; Kotz et al., 2009; Petacchi et al., 2005).

Therefore, in this study we sought to examine developmental changes in gray and white matter volume in the largest pediatric sample of developmental stuttering collected to date. These children were evaluated and scanned yearly for up to 4 years, a study design that allowed us to determine the eventual persistence or recovery of stuttering in each child and track developmental trajectories of their brain measures. For children in the persistent stuttering group (pCWS), we analyzed their structural magnetic resonance imaging (MRI) scans separately in two age groups based on the participant's age at each scan, one comprising those from 3 to 5 years of age (N = 42, 64 scans) and another, comprising those who fell within 6–12 years of age (N = 54, 112 scans). Our rationale for the separation of 3–5-year-olds (preschool-age) and 6–12-year-olds (school-age) was that they capture two critical stages of developmental stuttering. First, symptoms of stuttering typically start to appear during the preschool age, and spontaneous recovery of stuttering in this age range is still relatively high. On the other hand, children who continue to stutter during school-age are less likely to recover and this is the period when the transition to a chronic form of stuttering occurs in most children. The CWS were compared with age- and sex-matched controls who do not stutter, who reported no personal or family history of stuttering (N = 60, 91 scans for 3–5 years and N = 63, 139 scans for 6–12 years). We expected that examining the subset of children closest to the onset of stuttering (3–5 years) would provide the clearest clues to neural trait deficits associated with the onset of stuttering. Examining the subset of children in the older age range (6–12 years) would, on the other hand, provide information on later occurring changes that are linked to continued chronic stuttering. For the recovered group (rCWS), because the sample size was relatively small (N = 23, 64 scans), we analyzed all children in one group to examine morphology changes linked to neuroplasticity associated with natural recovery from stuttering during childhood.

Given previous studies of gray matter (Chang et al., 2008; Garnett et al., 2018; Koenraads et al., 2019) and white matter structure (Beal et al., 2013; Chow and Chang, 2017; Chang et al., 2015), and theoretical perspectives on neural deficits associated with persistent developmental stuttering (Chang and Guenther, 2020), we hypothesized that: a) early in development (preschool-age), children who eventually become persistent stutterers (pCWS) would exhibit gray and white matter morphometric differences from controls in structures comprising the BGTC network; b) later in development, pCWS exhibit both original and compensatory/adaptive additional changes compared to controls and rCWS; c) stuttering severity would be correlated with morphometric deficits associated with early stuttering and compensatory changes occurring in later stuttering; d) those rCWS would show normalization of morphometric differences found in pCWS, as well as possible compensatory signs in the regions supporting speech planning and timing (i.e., BGTC motor loop and the cerebellum).

2. Materials and methods

2.1. Study design and population

A total of 485 children between the ages of 3 and 10 were screened through an initial phone screening to assess whether they met basic inclusion criteria to participate in an ongoing longitudinal neuroimaging study to be followed for a period up to 4 years (see flowchart Supplemental Fig. S1 for details). Of those screened, a total of 278 children (150 CWS and 128 controls) were determined eligible and successfully completed the initial speech and language testing visit. Of those 278 children, 199 children (102 CWS and 97 controls) participated in at least one MRI scan session (Fig. S1). Each participant was scanned up to four times, with an inter-scan interval of approximately 1 year. The

age range for all visits was 3–12 years (12;11). The Institutional Review Board at Michigan State University approved of all procedures in the study. Subjects' consent was obtained according to the Declaration of Helsinki. All parents signed a written informed consent, and all children either provided verbal assent (non-readers; typically, 3–5-year-olds) or signed a written assent form (readers; typically, 6 years and older).

For this study, 470 high quality scans from 190 participants (95 CWS, 56 boys; 95 controls, 50 boys) were included in the final analyses, after excluding children whose MRI data was not useable due to excessive movement or incidental findings of abnormal brain structure. Incidental findings can range from normal variations in neuroanatomy to benign tumors, asymptomatic infarcts, and subclinical neurovascular pathology (Vernooij et al., 2007). Because these incidental findings were easily detected based on visual inspection, the abnormalities tended to cover a relatively large anatomical location and hence could have had the potential to influence the spatial normalization step of the VBM pipeline. Age at scan for each participant, showing the number of scans entered for each participant across groups for the 470 scans entered into the analysis are shown in Supplementary Figure 2 (Fig. S2). Number of datapoints entered for data analysis (1–4 longitudinal scans) for each group are shown in Table S2. Demographic information for the final group of participants can be found in Table 1. All participants were monolingual speakers of English who exhibited normal language and cognitive development as confirmed by detailed parent interviews that included review of speech-language developmental milestones and

Table 1
Participant characteristics in each age group (all subjects, 3–5-year-olds, and 6–12-year-olds).

Measure	Control	Persistent	Recovered
3:0–12:11 (all subjects)			
# Subjects	95	72	23
# Scans	230	176	64
Boy to girl ratio	50:45	44:28	12:11
Age at initial scan (month)	68.4 (21.1)	69.2 (20.6)	60.8 (20.7)
Age of stuttering onset (month)	N/A	34.3 (11.9)	32.9 (10.2)
SES1	6.22 (0.74)	6.11 (0.78)	6.04 (0.74)
IQ[2]	110.9 (13.1)	106.5 (13.6)[a]	108.7 (15.1)
SSI at initial visit	N/A	19.7 (6.5)	16.7 (5.9)
SSI at final visit	N/A	18.63 (7.0)	8.13 (3.1)[b]
3:0–5:11 (3–5 years old)			
# Subjects	60	42	18
# Scans	91	64	34
Boy to girl ratio	34:26	27:15	10:8
Age at initial scan (month)	55.2 (9.2)	54.4 (8.7)	51.1 (6.8)
Age of stuttering onset (month)	N/A	31.9 (9.9)	31.4 (8.3)
SES	6.22 (0.76)	6.20 (0.76)	5.92 (0.75)
IQ	110.1 (12.6)	108.3 (12.0)	111.3 (15.3)
SSI at initial visit	N/A	18.5 (5.5)	17.3 (5.2)
SSI at final visit	N/A	18.6 (5.8)	8.9 (2.9)[b]
6:0–12:11 (6–12 years old)			
# Subjects	63	54	14
# Scans	139	112	30
Boy to girl ratio	30:33	31:23	9:5
Age at initial scan (month)	84.6 (13.9)	84.9 (11.7)	83.5 (13.5)
Age of stuttering onset (month)	N/A	36.0 (12.5)	36.2 (11.2)
SES	6.23 (0.69)	6.10 (0.80)	6.3 (0.49)
IQ	113.7 (12.7)	106.5 (14.2)[a]	104.3 (14.1)[c]
SSI at initial visit	N/A	20.6 (6.7)	16.9 (7.1)
SSI at final visit	N/A	19.4 (7.4)	7.9 (3.2)[b]

1SES (Socioeconomic status) was calculated based on the Hollingshead Four Factor Index of Socioeconomic Status (Hollingshead, 1975 (Hollingshead, 1975)). In this study, a child's SES was measured based on the parent's (mother's) educational attainment, rated on a 7-point scale, e.g., a score of 6 indicates standard college or university graduation.
[2] Full-scale IQ calculated based on WASI (Wechsler Abbreviated Scale of Intelligence (Wechsler, 1999); ages 6 +) or WPPSI (Wechsler Preschool and Primary Scale of Intelligence (Wechsler, 2012); ages 3–5).
[a] Scores significantly lower in persistent than control group.
[b] Scores significantly lower in recovered than persistent group.
[c] Scores significantly lower in recovered than control group.

through a battery of speech, language and cognitive testing (see (Chow and Chang, 2017; Chang et al., 2015) for more details; see also Supplementary Table S1). Handedness was assessed using a modified Edinburgh handedness battery (Oldfield, 1971) and was similar between CWS (right: n = 76, left: n = 8, mixed: n = 9) and control groups (right: n = 80, left: n = 8, mixed: n = 9).

Within the stuttering group, stuttering severity was assessed using samples of spontaneous speech, elicited through storytelling and conversational tasks (and reading for children typically six and older who could read) with a parent and a certified speech-language pathologist (SLP). These samples were video-recorded and analyzed according to the procedure from the Stuttering Severity Instrument (SSI-4; (Riley, 2009)). The SSI-4 provides a composite stuttering severity rating based on frequency and duration of disfluencies occurring in the speech sample, as well as physical concomitants associated with moments of stuttering. To determine measurement reliability of the SSI-4 score ratings, an intraclass correlation coefficient (ICC = 0.97) was calculated based on two independent judges' ratings of SSI-4 from a subset of children's speech sample, indicating high reliability.

All CWS were diagnosed with stuttering during their initial visit by considering their composite SSI scores (=>10), %SLD (>3 %), expressed concern of the parent and clinician confirmation. In a few instances, some children exhibited SSI and SLD scores below the cut-off used to determine stuttering status (SSI<10 and/or %SLD<=3 %), however if their stuttering instances were qualitatively consistent with stuttering and both parent and clinician reports pointed to stuttering, the child was entered into the study as a child who stutters. On the other hand, a handful of control participants showed %SLD exceeding 3 %, but the SLDs were qualitatively inconsistent with stuttering (e.g., easy repetitions of words rather than sound/syllable repetitions and no prolongations/blocks). If neither the parent nor SLP expressed concern and no family history of stuttering reported, such a child was entered as a control participant.

The CWS were later categorized as recovered or persistent through a combination of measures acquired in subsequent visits. Specifically, a child was categorized as persistent if the SSI-4 score was equal or greater than 10 (corresponding to 'very mild' in SSI-4 severity classification) at the second visit or thereafter, and the onset of stuttering had been at least 36 months prior to his most recent visit. A child was considered recovered if the composite SSI-4 score was below 10 at the second visit or thereafter. Determination of recovery status also required the consideration of percent occurrence of stuttering-like disfluencies (% SLD) in the speech sample (>3 for persistent) as well as clinician and parental reports. Parents were interviewed each year to report on their children's stuttering status as observed in the home setting and other environments. Similar criteria were used to determine persistence versus recovery in stuttering children in previous studies (Yairi and Ambrose, 1999; Yairi et al., 1996).

In cases where persistence versus recovery status remained unclear during the final visit, the stuttering participants' speech status was checked via parent phone interview 1–2 years post final visit to track and document any changes in the child's recovery or persistent status. Using these criteria, we identified 72 pCWS and 23 rCWS in the final analyses.

2.2. MRI data acquisition

Anatomical images were acquired on a GE 3 T Signa scanner (GE Healthcare) with an 8-channel head coil at Michigan State University. In each scan session, a whole brain 3D inversion recovery fast spoiled gradient-recalled T1-weighted images with cerebrospinal fluid suppressed was obtained using the following parameters: echo time = 3.8 ms, repetition time = 8.6 ms, inversion time = 831 ms, inversion repetition time = 2332 ms, flip angle = 8°, and receiver bandwidth = 620.8 kHz. As part of the longitudinal imaging study, DTI and resting state functional MRI data were also collected but they are not reported in

the current article. Previous studies have reported results from datasets collected from subsets of participants in the current study (shown in Table S3). DTI datasets from a subset of participants have been reported in three previous papers (Chang et al., 2015; Chang and Zhu, 2013; Johnson et al., 2022; Neef et al., 2022). Resting state fMRI datasets from a subset of participants were also reported in previous studies (Chang and Zhu, 2013; Chang et al., 2016, 2018). These previous studies reported imaging findings from a different imaging modality than what is reported in the current study. With regard to studies that used T1 datasets as is reported in the current study, one previously published study reported cortical thickness (Garnett et al., 2018) and another reported on the relationship between gray matter volume and expression patterns of stuttering-related genes (Chow et al., 2020). All these previous studies only included approximately half the number of subjects that are reported in the current study (Table S3).

All children were trained with a mock MRI scanner to familiarize them with the MRI environment and procedures, and to practice keeping still while lying down inside the bore. Recordings of MRI scanning noises were played during this session, so that children were aware of the loud MRI sounds during scanning. During the MRI-scan visit, children viewed a movie to help them stay still, and a research staff member sat next to the child if needed to ensure comfort and compliance throughout the scanning procedure.

2.3. Voxel-based morphometry (VBM)

Voxel-Based Morphometry (VBM) analysis was conducted using the CAT12 toolbox (http://www.neuro.uni-jena.de/cat/). CerebroMatic Toolbox was used to create the study-specific templates based on an large publicly available data set and the demographic features (age and sex) of the participants in the current study (Wilke, 2018). Volume of each voxel were obtained by multiplying (or modulating) tissue probability by the deformation field derived from the DARTEL normalization procedure (Ashburner, 2007). Individual, modulated images were resampled to 1.5 mm isotropic voxels and spatially smoothed with a Gaussian kernel with FWHM of 6 mm. To account for the dependence of participants' multiple scans in the current study, gray matter volume (GMV) and white matter volume (WMV) images were analyzed separately using Sandwich Estimator, which was designed for analyzing longitudinal and repeated measures data and has been shown to be robust to missing data and unbalanced designs (Guillaume et al., 2014; Ibrahim and Molenberghs, 2009). Because the sample sizes of the previous VBM studies of children who stutter (CWS) were relatively small, and this is the first time preschool aged CWS were studied, we did not make assumptions that the structural differences were in specific areas or limit our analyses to certain regions of interest. For each age group, the model included group (pCWS, rCWS and controls) and sex as factors, group by age interaction, and quadratic age, IQ, intracranial volume, socioeconomic status (SES) and stuttering severity as covariates to control potential sources of variations. We included quadratic age as a covariate and do not report it separately (however, we show in Fig. S4 non-linear age effects found in our data, which complement the main linear age effects findings) as our main interest was to examine linear age effects. Examining linear age effects was a focus given our previously reported finding of linear (but not non-linear) effects in white matter structural data (Chow and Chang, 2017) and given previous longitudinal studies of gray matter development encompassing large age ranges across the lifespan that have reported primarily linear age effects found within the age range of our participants (3–12 years) (Gogtay and Thompson, 2010; Mills et al., 2016). Voxel-wise t-statistics of the group differences were calculated. Voxel-wise height threshold $p < 0.005$ and cluster-size threshold $k > 457$ voxels in GMV analysis, and $k > 318$ voxels in WMV analysis were used to control for false positives. This set of thresholds resulted in a corrected $p < 0.05$. The cluster-size threshold was determined by AFNI 3dClustSim (version 17.2.13) with non-Gaussian auto-correlation function (-acf option) (Cox et al., 2017).

2.4. Data availability

The datasets generated and/or analyzed in the current study are available from the corresponding author upon reasonable request.

3. Results

3.1. Participant characteristics

The pCWS, rCWS and fluent controls did not differ significantly in sex ratios, age at the initial scan, or SES (Table 1). There were no significant differences between pCWS and rCWS in onset age of stuttering or stuttering severity at the initial visit. As expected, stuttering severity was significantly lower in rCWS than pCWS at the final visit. Compared to controls, pCWS scored significantly lower on IQ than controls based on the combined age groups (total) and school-age subjects, while rCWS only scored significantly lower on IQ in the analyses of school-age subjects. It is important to note that the mean IQ scores in both pCWS and rCWS were well within the normal range. The differences in IQ were driven by above-average IQ in the control group. Given these differences, we entered IQ as a covariate in our statistical analyses.

3.2. Morphometric anomalies associated with persistent stuttering in preschool-age children

The key neuroimaging findings are shown in figures and described in the text below; results of all contrasts are listed in Supplementary Table S3.

3.3. Overall differences (group effects) between pCWS and controls

Significant differences between pCWS and controls were found in gray (Fig. 1 A) and white matter volume (Fig. 1B). In this preschool age range (3–5 years), pCWS exhibited reduced GMV compared to controls in the putamen and the nucleus accumbens. In terms of white matter, decreased WMV was observed in white matter tracts encompassing the bilateral corona radiata, superior longitudinal fasciculi (SLF) and the corpus callosum for pCWS relative to controls (Fig. 1B).

3.4. Developmental trajectory differences (age effects) between pCWS and controls

In addition to group effects, we investigated whether there were significant group by age interactions, reflecting differences in developmental trajectories between groups. In the preschool age group, differences were only observed in the development of WMV but not GMV when comparing pCWS with controls (Fig. 2). Decreasing WMV was observed in white matter tracts encompassing the bilateral corona radiata and SLF, including the white matter near the left ventral premotor area for pCWS, while WMV in these areas were increasing for controls. In addition, lower WMV growth rates were found for pCWS in the corpus callosum and the inferior longitudinal fasciculus (ILF).

3.5. Morphometric anomalies associated with persistent stuttering in school-age children

3.5.1. Overall differences (group effects) between pCWS and controls
Fig. 3 shows results from the group contrast between pCWS and controls in the school-age range. In this older age group, GMV in the thalamus was significantly reduced in pCWS compared to controls (Fig. 3 A). Regarding WM, pCWS exhibited smaller volume in white matter tracts encompassing the corona radiata, SLF and the internal capsule relative to controls (Fig. 3B).
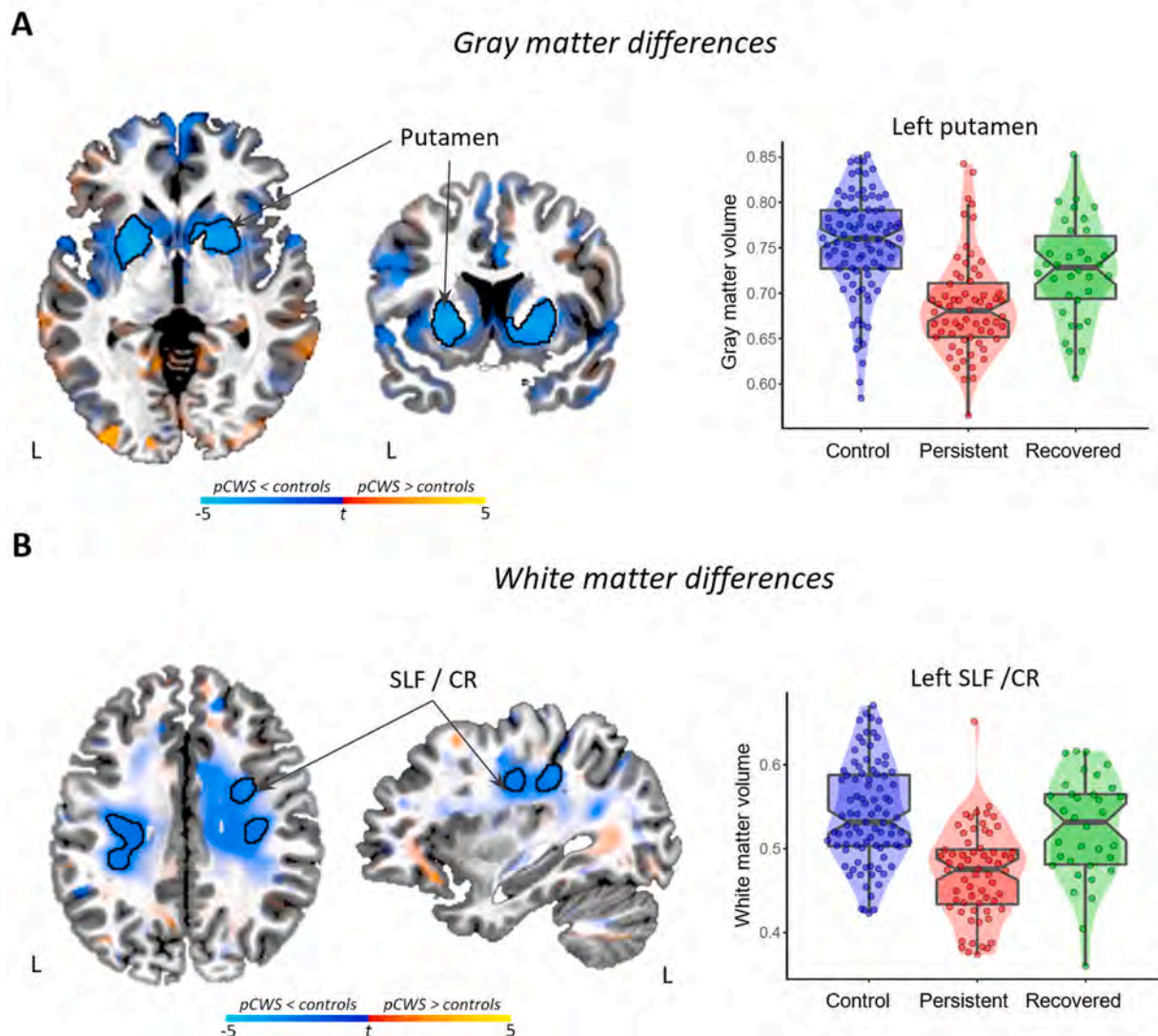
Fig. 1. Differences between preschool-age children with persistent stuttering and controls (3–5 years old) in gray matter volume (A) and white matter volume (B). In the left panel, between-group differences are overlaid on a single subject anatomical image. Orange and blue indicate increased and decreased volume at uncorrected $p < 0.05$, respectively. Clusters exhibiting a significant difference at corrected $p < 0.05$ are outlined by black lines. In right panel, violin plots illustrate the group differences around the peak of a significant cluster. Each marker represents the modulated volume values averaged across voxels around the peak location in each scan. The values were adjusted for the effects of sex, age, IQ, intracranial volume and socioeconomic status. SLF: superior longitudinal fasciculus, CR: corona radiata.

3.5.2. Developmental trajectory differences (age effects) between pCWS and controls

For pCWS relative to controls in the school-age range, the GMV growth rate was lower in the left IFG and the insula as well as the calcarine gyrus in the visual cortex, whereas GMV growth rate was higher in the precuneus (Fig. 4 A). PCWS also showed greater growth rates compared to controls in white matter areas including the body and isthmus of the corpus callosum and the WM near the right dentate nucleus (Fig. 4B).

3.6. Morphometric anomalies associated with persistent stuttering from the entire sample of children

The comparison between pCWS and controls including all children (ranging from preschool-age to school-age children) showed significant decreases in GMV for pCWS in the left ventral premotor cortex (vPMC) and the nucleus accumbens (Fig. 5 A). In addition, pCWS showed

decreased GMV with age in the hippocampus and GMV in the right posterior middle temporal lobe; in contrast, controls showed increased volume with age in both areas (Fig. 5B).

3.7. Association between brain volume and stuttering severity in children with persistent stuttering

In the preschool-age group, WMV in the bilateral corona radiata, corpus callosum (genu, mid body and splenium), and the right AF in the temporal lobe (not shown) was negatively associated with stuttering severity, but no significant association between stuttering severity and GMV was found. By contrast, in the school-age group, significant association with stuttering severity was only found in gray matter areas, including in the bilateral nucleus accumbens and the right cerebellar lobule VI (Fig. 6). Apart from stuttering severity, we did not find significant association between gray or white matter and other covariates (IQ and SES) nor sex by group interaction.
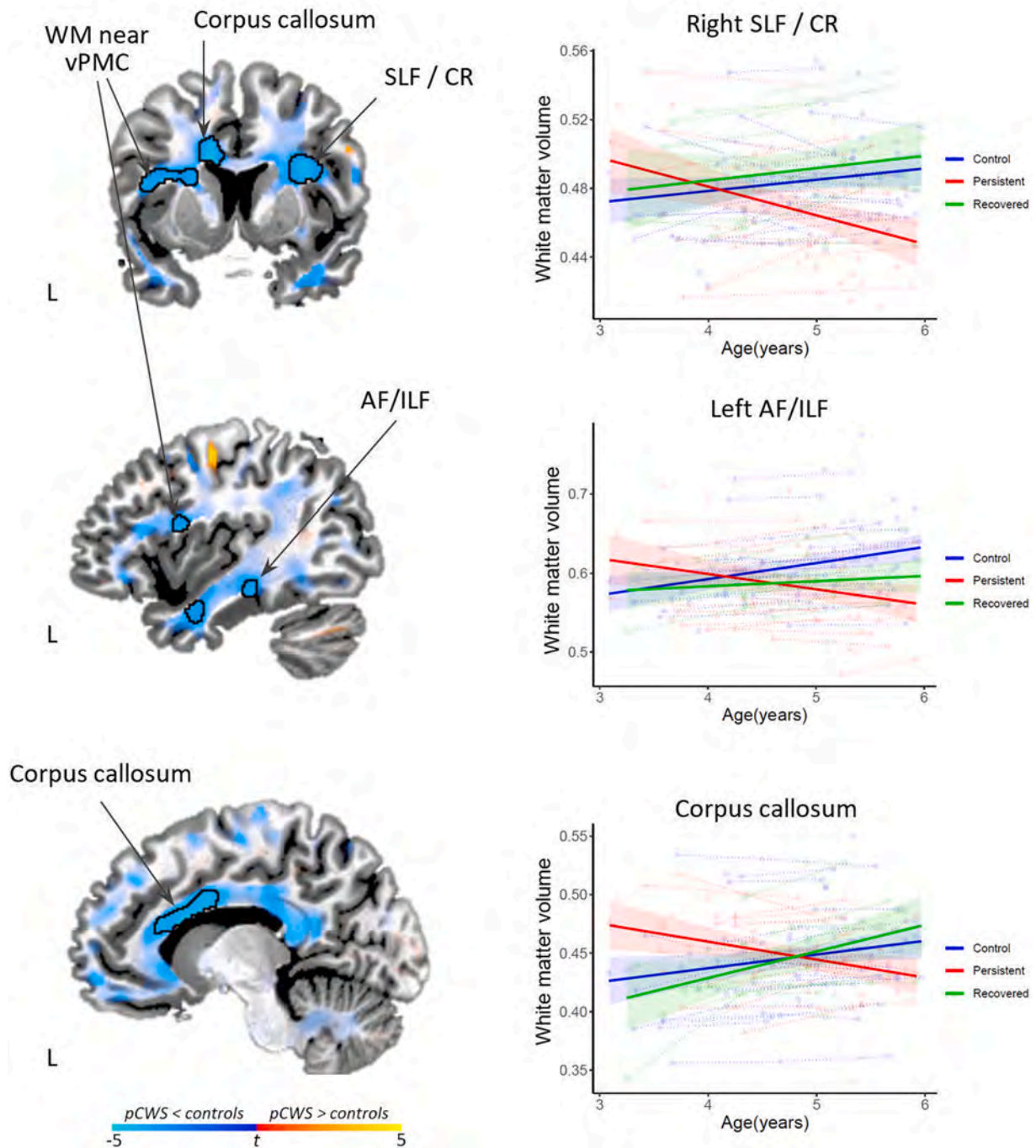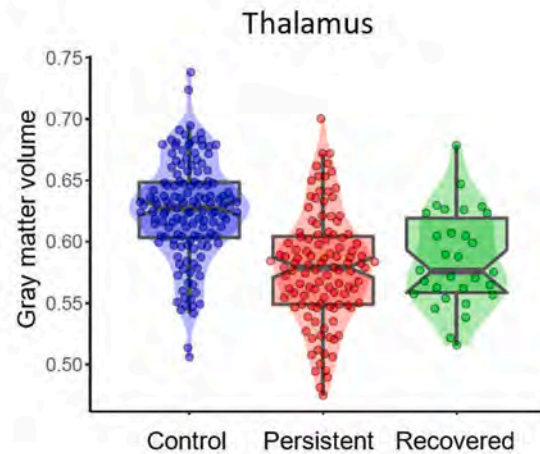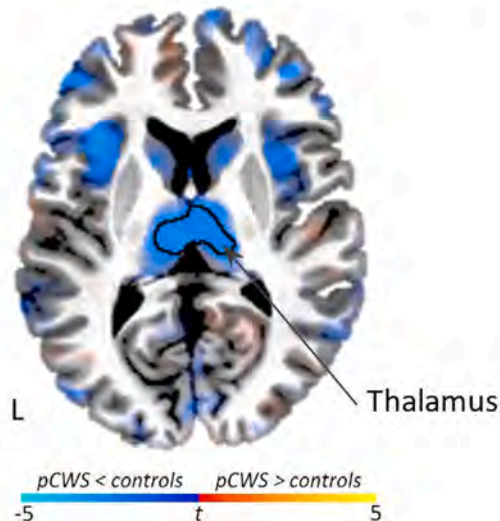
Fig. 2. Differences between school-age children with persistent stuttering and controls (3–5 years old) in growth rate of white matter volume. In the left panel, between-group differences in growth rate are overlaid on a single subject anatomical image. Orange and blue indicate increased and decreased growth rate at uncorrected $p < 0.05$, respectively. Clusters exhibiting a significant difference at corrected $p < 0.05$ are outlined by black lines. In the right panel, individual volume measures are plotted against age to illustrate the age-related changes in each group around the peak of a significant cluster. Each marker represents the modulated volume values averaged across voxels around the peak location in each scan. The values were adjusted for the effects of sex, IQ, intracranial volume and socio-economic status. Longitudinal volume measures of a participant are connected using dotted lines. Solid lines represent the best-fit linear trend line in each group and the shaded areas represent the standard error of the trend line. SLF: superior longitudinal fasciculus, CR: corona radiata, AF; arcuate fasciculus, ILF: inferior longitudinal fasciculus.
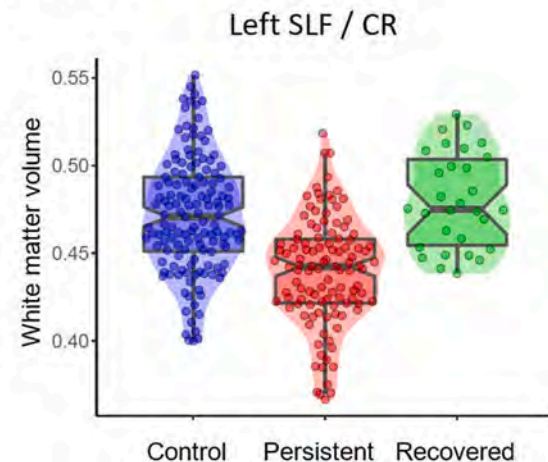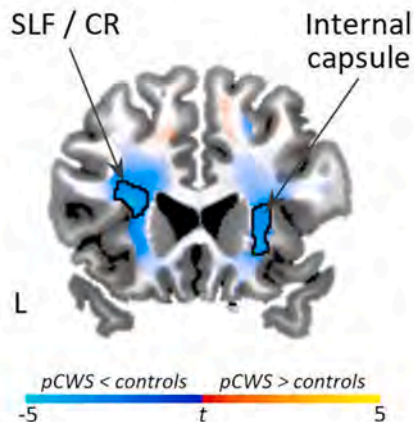
Fig. 3. Differences between older children with persistent stuttering and controls (6–12 years old) in gray matter volume (A) and white matter volume (B). In the left panel, between-group differences are overlaid on a single subject anatomical image. Orange and blue indicate increased and decreased volume at uncorrected $p < 0.05$, respectively. Clusters exhibiting a significant difference at corrected $p < 0.05$ are outlined by black lines. In right panel, the violin plots illustrate the group differences around the peak of a significant cluster. Each marker represents the modulated volume values averaged across voxels around the peak location in each scan. The values were adjusted for the effects of sex, age, IQ, intracranial volume and socioeconomic status. SLF: superior longitudinal fasciculus, CR: corona radiata.

3.8. Morphometric findings associated with recovery from stuttering

Compared to controls, rCWS exhibited a lower growth rate in the left insula/inferior frontal area (Fig. 7 A). On the other hand, a higher growth rate in rCWS relative to controls were observed in extensive white matter areas including the bilateral corona radiata, SLF, corpus callosum, left AF, and bilateral cerebellar peduncles around the dentate nuclei (Fig. 7B).

4. Discussion

The current study is the first longitudinal study that examined brain development trajectories associated with persistence and recovery of stuttering during childhood, encompassing both preschool-age (3–5 years of age) and school-age (6–12 years of age) children. The preschool-age group is particularly important for understanding the etiology of stuttering because it coincides with the typical onset time of stuttering. The results indicate that stuttering persistence is associated with wide-ranging structural anomalies, including in major structures of the BGTC loop, the left perisylvian speech language networks, the
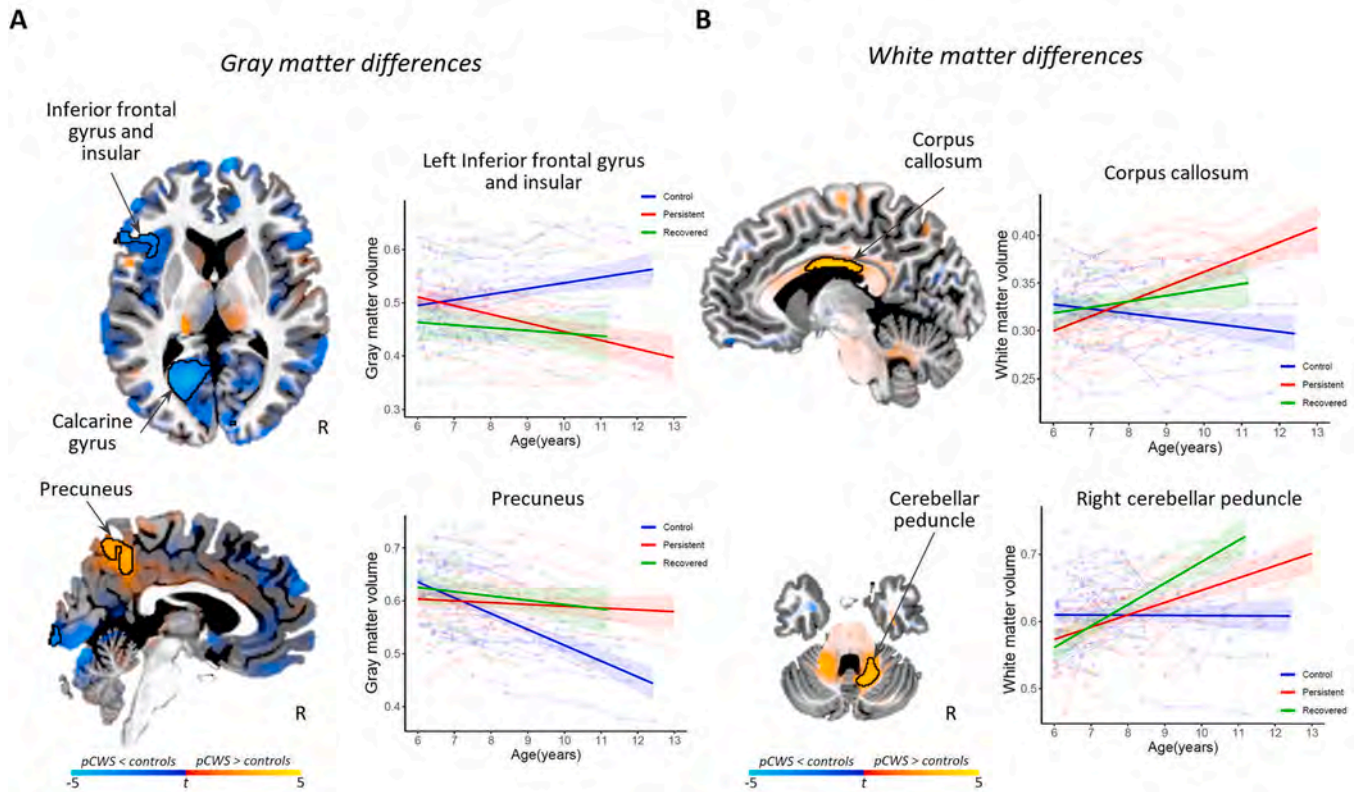
Fig. 4. Differences between older children with persistent stuttering and controls (6–12 years old) in growth rate of gray matter volume (A) and white matter volume (B). Between-group differences in growth rate are overlaid on a single subject anatomical image. Orange and blue indicate increased and decreased growth rate at uncorrected $p < 0.05$, respectively. Clusters exhibiting a significant difference at corrected $p < 0.05$ are outlined by black lines. In the scatter plots, individual volume measures are plotted against age to illustrate the age-related changes around the peak of a significant cluster in each group. Each marker represents the modulated volume values averaged across voxels around the peak location in each scan. The values were adjusted for the effects of sex, IQ, intracranial volume and socio-economic status. Longitudinal volume measures of a participant are connected using dotted lines. Solid lines represent the best-fit linear trend lines in each group and the shaded areas represent the standard errors of the trend lines.

cerebellum and white matter tracts that interconnect these regions. Some of these morphometric variations across subjects were associated with stuttering severity, which further supports the pivotal role of the speech motor system in stuttering persistence. However, the patterns of structural anomalies appear to differ between preschool- and school-age pCWS. In preschool-age children, the most significant morphometric difference in pCWS relative to controls were in the bilateral putamen and nucleus accumbens, and in the white matter tracts that interconnect speech-language and motor areas such as the SLF and motor projection fibers. On the other hand, in school-age children, the main difference between pCWS and controls become evident in the thalamus and the white matter in the internal capsule, corona radiata and the SLF. The most prominent gray matter anomalies appeared to transition from regions receiving cortical projections in the BG (i.e., the putamen) at younger ages, to the region receiving output from the BG (i.e., the thalamus) at older ages. However, this dynamic developmental change could be the result of the interaction between stuttering-related anomalies and normal brain developmental processes such as the observation that GMV in many regions decreases with age in school-age children. It has been shown that GMV in many parts of the brain decrease with age, especially after the age of seven (Gogtay et al., 2004; Sowell et al., 2003; Tamnes et al., 2017).

While stuttering persistence was mainly associated with decreased gray and WMV or an attenuated growth rate in the speech-motor structures, recovery from stuttering was primarily associated with increased growth rate of white matter volume in tracts connecting these

structures, suggesting that these increases reflect a process of compensation for the neural deficits in stuttering. These main findings are elaborated and discussed below.

4.1. Early involvement of BGTC structures associated with persistent stuttering

One strength of the current investigation was that, due to the relatively large sample size analyzed, we were able to examine children close to typical stuttering onset (3–5 years) and those who had been stuttering for longer periods (6–12 years) separately. In the preschool-age group, we found that compared to controls, CWS who eventually develop persistent stuttering (pCWS) had significant GMV decreases relative to controls in the bilateral putamen and nucleus accumbens (Fig. 1 A). This GMV decrease in preschool-age pCWS was accompanied by reduced overall volume and growth rate in major white matter structures including the corpus callosum, corona radiata, SLF and ILF (Fig. 1B and Fig. 2). While the corona radiata and corpus callosum are known to be associated with motor projection fibers and interhemispheric connections respectively, ipsi- and contralateral corticostriatal projection fibers also pass through these structures (Shepherd, 2013). Given the gray matter anomalies in the striatum, the white matter anomalies in preschool-age CWS may also reflect connectivity deficits involving the BG. In addition, reduced WMV growth rate was found in the bilateral SLF near the vPMC and the ILF (Fig. 2). These white matter tracts are involved in transmitting speech sound representations,
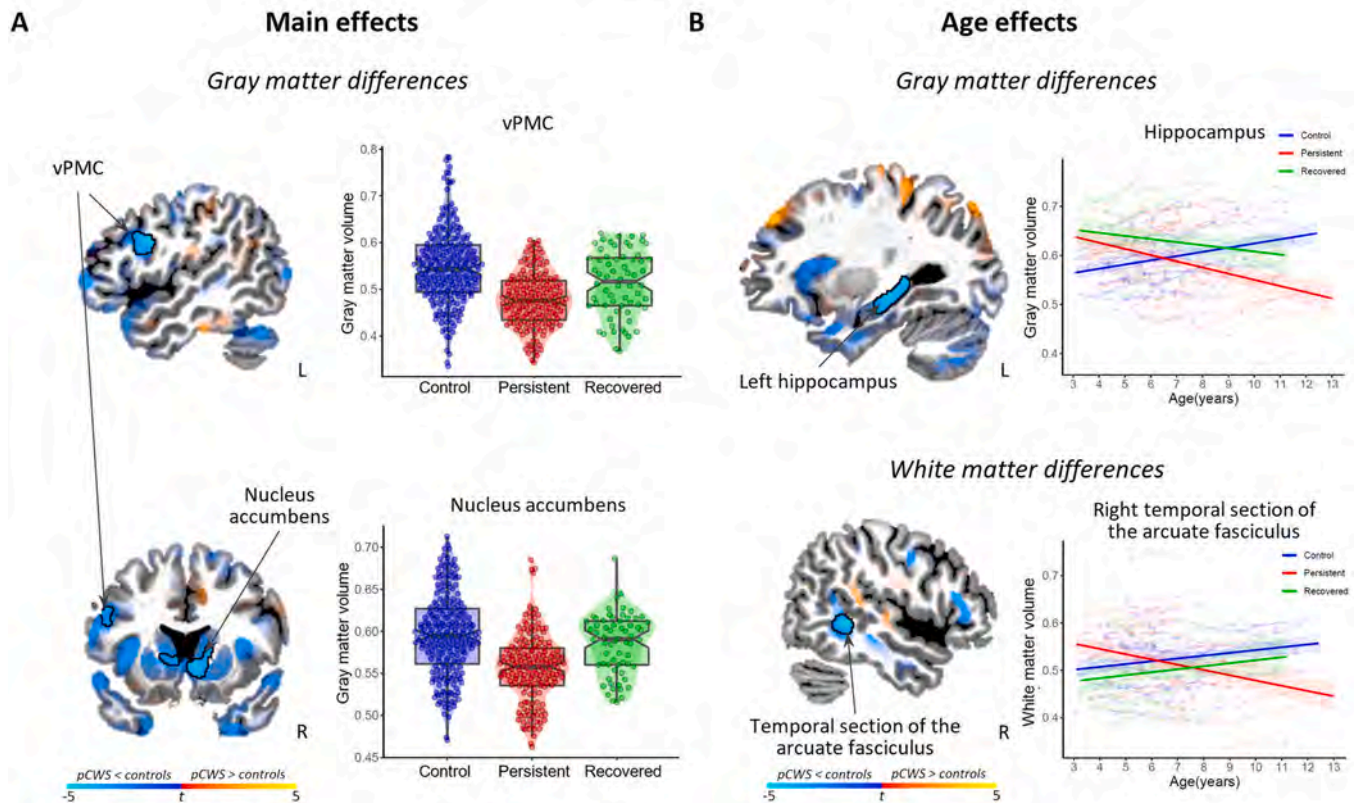
Fig. 5. Differences between children with persistent stuttering and controls when scans from all subjects from age 3–12 years old were analyzed together in a single model. (A) Between group differences in gray matter volume are overlaid on a single subject anatomical image. Orange and blue indicate increased and decreased volume at uncorrected $p < 0.05$, respectively. Clusters exhibiting a significant difference at corrected $p < 0.05$ are outlined by black lines. The violin plots illustrate the group differences around the peak of a significant cluster. The values were adjusted for the effects of sex, age, IQ, intracranial volume and socioeconomic status. (B) Between group differences in growth rate of gray matter are overlaid on a single subject anatomical image. The scatter plots illustrate the growth rate differences around the peak of a significant cluster in each group. Each marker represents the modulated volume values averaged across voxels around the peak location in each scan. The values were adjusted for the effect of sex, IQ, intracranial volume and socioeconomic status. Longitudinal volume measures of a participant are connected using dotted lines. Solid lines represent the best-fit linear trend lines in each group and the shaded areas represent the standard errors of the trend lines. vPMC: Ventral premotor cortex.

providing inputs to the BGTC loop (Hickok, 2012). Taken together, GMV and WM anomalies observed in preschool age pCWS suggest that deficits in the BGTC motor loop plays an important role in the onset and persistence of stuttering behaviors. This notion is also supported by the negative association between stuttering severity and WMV in the corpus collosum, SLF and corona radiata in preschool-age pCWS (i.e., lower the volume, higher the severity, Fig. 6 A). While the negative association between putamen and nucleus accumbens volume and stuttering severity was not significant in preschool-age CWS, it was significant in school-age pCWS (Fig. 6B).

Previous studies reported reduced volume in the putamen in school-age CWS (Beal et al., 2013; Foundas et al., 2013). Moreover, white matter anomalies in the corpus collosum, SLF, corona radiata and AF/ILF observed in the current study are consistent with the previous DTI studies of school-age pCWS, which reported decreased fractional anisotropy in those white matter areas (Chow and Chang, 2017; Chang et al., 2015). These structural anomalies may be associated with weaker connectivity between the putamen and several cortical regions, including the left insula, IFG and middle frontal gyrus and supplementary motor area (SMA) in pCWS, perhaps reflecting either decreased efficiency, or under-utilization of these connections (Chang and Zhu, 2013; Chang et al., 2016; Kronfeld-Duenias et al., 2016). The current results provide empirical support for possible deficits in cortical-BG connections in stuttering, and that these deficits seem to be present

early, near onset of stuttering. If connectivity within the BGTC circuit is not well developed, timing of motor sequences could be disrupted, which results in a mismatch between sensory targets and motor representations (Guenther, 2016, 2006).

In previous structural MRI studies of stuttering, the left IFG/vPMC region has been repeatedly reported to differentiate stuttering speakers from controls (Beal et al., 2013; Chang et al., 2008, 2015; Civier et al., 2015; Connally et al., 2014; Kell et al., 2009; Sommer et al., 2002; Watkins et al., 2008). The left IFG/vPMC corresponds to the speech sound map area in the DIVA model (Directions into Velocities of Articulators) (Guenther, 2006), a critical area that is part of both feedforward and feedback pathways within the model that interconnects with several cortical and subcortical regions. The DIVA model provides a neurocomputational modeling framework to mechanistically interpret the neuroimaging findings from this study. Structurally, the inferior frontal/vPMC region has major connections with motor cortices and the sensory cortical areas via the SLF, language areas via the arcuate fasciculus and the SMA via the frontal aslant tract (Kronfeld-Duenias et al., 2016; Catani et al., 2005; Dick et al., 2019). The left vPMC is thus an important hub area within the BGTC loop in speech production that is linked to two of the three main loci within the BGTC loop that are posited to be affected in stuttering (i.e., impairment of axonal projections between cortex, BG, and thalamus; PDS2 and corticocortical connections; PDS3) (Chang and Guenther, 2020).
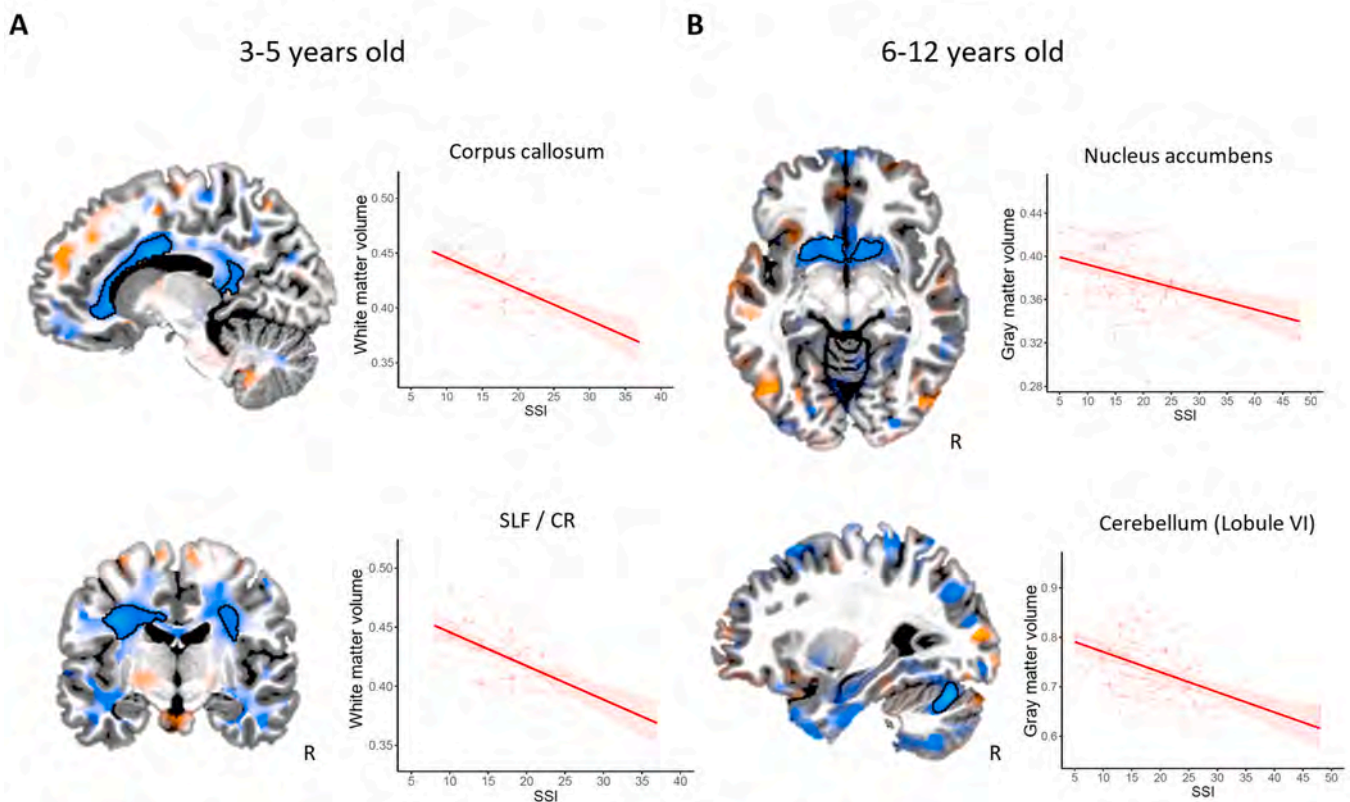
Fig. 6. Associations between gray/white matter volume and stuttering severity scores in children who stutter from age 3–5 years old (A) and 6–12 years old (B). Estimated association between stuttering severity and volume measures in each voxel is overlaid on a single subject anatomical image. Orange and blue indicate positive and negative association at uncorrected $p < 0.05$, respectively. Clusters exhibiting a significant association at corrected $p < 0.05$ are outlined by black lines. In the scatter plots, individual volume measures around the peak of a significant cluster are plotted against stuttering severity scores. Each marker represents the modulated volume values averaged across voxels around the peak location in each scan. The values were adjusted for the effect of sex, age, IQ, intracranial volume and socioeconomic status. Longitudinal volume measures of a participant are connected using dotted lines. Solid lines represent the best-fit linear trend lines in each group and the shaded areas represent the standard errors of the trend lines.

Specifically, we found evidence of reduced left vPMC volume based on the group contrasts of pCWS and controls across the whole age range tested (Fig. 5 A). When examining within the separate younger and older groups, however, this decreased left vPMC volume did not reach significance for group effects (see Fig. 3 A). Significant age effects were nevertheless found in this region, whether it was in the preschool-age group in terms of white matter encroaching on the left vPMC region (Fig. 2) or in terms of GMV in this area for the school-age groups (Fig. 4). These results suggest that the reduced vPMC GMV found in school-age may be associated with reduced connections to the region during younger ages. We further discuss how our findings can be interpreted in the context of the DIVA model under the neuroanatomical accounts section below.

4.2. Emergence of thalamus anomalies in school-age children with persistent stuttering

While reduced volume of the structures supporting the corticostriatal projections as well as the input regions of the BG such as the putamen appear to be the hallmark of preschool-age pCWS, the most prominent structural anomalies associated with school-age pCWS were in the thalamus. In the BGTC loop, the thalamus receives projections from the BG and projects to the cortical motor areas. It also has bidirectional direct connections with the cerebellum and modulates functions of the BG and the cerebellum (Bostan and Strick, 2018; Chen et al., 2014). The

decreased GMV in the thalamus may affect both the BGTC and cerebellar processes important for speech-motor control (Kotz and Schwartze, 2010; Kotz et al., 2016). The thalamus anomalies could arise due to deficits occurring earlier in the putamen where structural anomalies were observed in preschool-age pCWS (Wu and Hallett, 2013). It also indicates that structural anomalies associated with persistent stuttering are not static; they may develop in tandem with the progression of the disorder. On the other hand, reversing this anomalous brain development or enhancing compensatory process may reduce stuttering severity or even facilitate recovery.

Interestingly, reduced putamen volume observed in the younger pCWS was not observed in the older age group. However, we believe that this negative result does not imply that the anomaly in the putamen is normalized, for two reasons. First, in the school-age pCWS, putamen and nucleus accumbens volume was negatively correlated with stuttering severity (Fig. 6B), indicating the functional importance of these structures in stuttering behaviors. Second, the reduction of volume in the putamen and possibly many other regions may become less evident due to normal development of gray and white matter. It has been shown that GMV in many parts of the brain decrease with age, especially after the age of seven (Gogtay et al., 2004; Sowell et al., 2003; Tamnes et al., 2017). Our data also showed that GMV of controls decreased in most of the cortical and subcortical areas including the putamen. If the GMV reduction in normal development is delayed in pCWS, that is, GMV reduction occurs at a lower rate relative to controls, the effect of lower
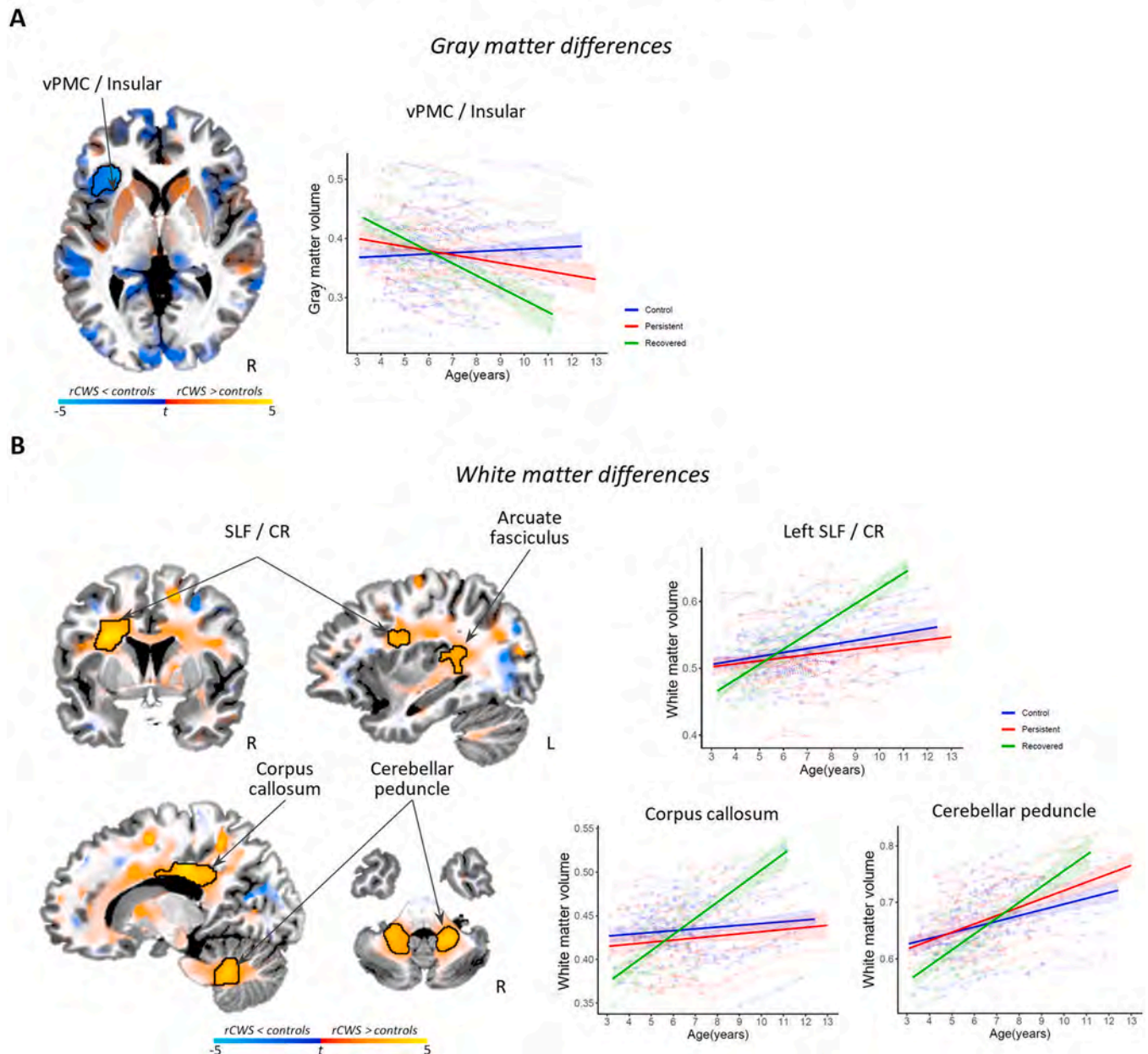
Fig. 7. Differences between children who recovered from stuttering and controls when scans from all participants from age 3–12 years old were analyzed together in a single model. Between group differences in growth rate of gray matter volume (A) and white matter volume (B) are overlaid on a single subject anatomical image. Orange and blue indicate increased and decreased volume at uncorrected $p < 0.05$, respectively. Clusters exhibiting a significant difference at corrected $p < 0.05$ are outlined by black lines. The scatter plots illustrate the growth rate differences around the peak of a significant cluster in each group. The values were adjusted for the effects of sex, IQ, intracranial volume and socioeconomic status. Each marker represents the modulated volume values averaged across voxels around the peak location in each scan. Longitudinal volume measures of a participant are connected using dotted lines. Solid lines represent the best-fit linear trend lines in each group and the shaded areas represent the standard errors of the trend lines. vPMC: Ventral premotor cortex, SLF: superior longitudinal fasciculus, CR: corona radiata.

GMV in the putamen in preschool-age pCWS will be diminished in the older age range, as illustrated in Fig. S3. If these trends continue, this may also explain why several studies reported that adults with persistent stuttering showed greater GMV in the left putamen compared to adults who do not stutter (Lu et al., 2010; Montag et al., 2019; Neef et al., 2018). This interplay between stuttering-related anomalies and normal brain development shows the importance of studying finer-grained age groups to reveal the complexity of the neural development in pCWS.

4.3. White matter volume increases are associated with stuttering recovery

Similar to pCWS vs controls (Fig. 5), rCWS showed decreased GMV in the ventral premotor area and insula relative to controls when we included all the scans in the whole age range in the analysis (Fig. 7 A). Different from pCWS vs controls, decreased volume in the BG and the thalamus was not found in rCWS vs controls. This qualitative difference may indicate that the causes of stuttering in pCWS and rCWS have different neuroanatomical origins. However, direct comparison between pCWS and rCWS did not show any significant group differences in these

subcortical areas (Supplementary Table S3). RCWS may have more confined deficits associated with corticostriatal connections while pCWS may have more widespread anomalies throughout the BGTC network. However, it is also possible that the deficits associated with the BG and the thalamus had resolved in pre-school age CWS or we did not have sufficient statistical power to detect the deficit due to the small number of rCWS in the current study.

A marked difference between pCWS and rCWS is that the growth rate was significantly higher for rCWS in several WM areas (Fig. 7B) where decreased volume or growth rate was observed in preschool- and school-age pCWS, including in the left corona radiata, the corpus callosum, SLF and the left AF (Figs. 1B, 2 & 3B). This observation was supported by direct comparison between pCWS and rCWS in age effects, which showed a significant group by age interaction in those areas (Supplementary Table S3). This divergent development in pCWS and rCWS has also been reported in a longitudinal DTI study (Chow and Chang, 2017) that examined a subset of the same participants included in the current study and strongly suggests that the WMV increases underlie a possible normalization or compensatory process associated with natural recovery from stuttering.

Increased growth rate in the bilateral cerebellar peduncle around the dentate nucleus was also observed in rCWS (Fig. 7B). This is an interesting result because, different from other WM areas showing increased WM growth rate in rCWS, decreased volume or growth rate in the bilateral cerebellar peduncle around the dentate nucleus was not observed in pCWS. Instead, increased growth rate in the right cerebellar peduncle around the dentate nucleus as well as the corpus callosum was found in school-age pCWS, but the spatial extent is less than that observed in rCWS. This may indicate that increased growth rate in the cerebellar peduncle is associated with an incomplete compensatory process associated with stuttering regardless of persistence or recovery. The growing volume of the cerebellar peduncle also indicates the involvement of the cerebellum in compensatory process. This notion is further supported by the observation of negative association between the right cerebellum lobule VI and stuttering severity in school-age pCWS (Fig. 6B). Overall, our results indicate that the cerebellum may support increased fluency, but it is insufficient to support complete recovery from stuttering. Rather, as discussed in an earlier section, recovery from stuttering may require compensation involving the BGTC loop.

4.4. An updated neuroanatomical account of childhood stuttering persistence and recovery

The current results corroborate many predictions of a neuroanatomical model of speech motor control, the DIVA model (Guenther, 2016, 2006). In theorizing of potential impairments in persistent developmental stuttering (PDS), Guenther (Guenther, 2016) proposes three possible locations of impairments in the BGTC loop (also described in (Chang and Guenther, 2020)). The first is in the basal ganglia proper (PDS-1), the second is the corticostriatal projections from cerebral cortex to the basal ganglia (PDS-2), and the third is the network of cortical regions that process cognitive and sensorimotor aspects of speech (PDS-3). The current finding of early presence of decreased GMV in the putamen and nucleus accumbens in pCWS supports PDS-1, and the decreased WMV that appear to intersect with the corticostriatal tracts within the motor projection fibers and the corpus callosum supports PDS-2. In addition, evidence for PDS-3 was also found, specifically relating to WMV decreases observed in the inferior frontal areas, SLF and AF/ILF in the left hemisphere. These WMV reductions may reflect either decreased efficiency, or under-utilization of left frontotemporal connections that enable auditory-motor integration needed for fluid speech motor control. Overall, our results support all three possibilities hypothesized in (Guenther, 2016). However, further research is needed to understand the contribution of these three structures to the onset and persistence of stuttering and their specific effects on stuttering behaviors.

Guenther (Guenther, 2016) questioned whether the weakened corticostriatal connectivity reported in CWS was a secondary consequence of impairment elsewhere rather than the root cause of stuttering, given that this finding had not been consistently found in adult speakers who stutter. The current findings in young children including those in preschool-age point to differences in corticostriatal connectivity as critical loci of impairment associated with stuttering. The lack of consistent findings of BGTC anomalies reported in older children and adults who stutter from previous studies may have been influenced by the effects of later occurring structural development that obscure earlier group differences (e.g., normal decreases in GMV in controls that occur later in development that could then become similar to the level of low GMV in stuttering speakers; see Fig. S3 for example), as well as possibly the compensatory processes developed later in life. More longitudinal studies involving younger children close to stuttering onset will be needed to address this question further.

The current observation of significantly reduced GMV in the putamen and nucleus accumbens (NAcc) in the earliest stages of stuttering (in preschool-age CWS) is a novel finding that lends support for the crucial role of the basal ganglia and the dopamine system in speech and stuttering (reviewed in (Alm, 2021)). The dopamine system underlies our ability to learn and execute rapid, automatized movement sequences (Goerendt et al., 2003; Tremblay et al., 2010) and has been linked to stuttering due to related pharmacological effects in stuttering (Maguire et al., 2002; Wu et al., 1997). The striatum, comprising the basal ganglia structures caudate, putamen, and NAcc, receives input from most parts of the cerebrum, is a major target for dopamine. Relevant to the findings of the current study, dopaminergic neurons from the substantia nigra pars compacta (SNc) project to the putamen (sensorimotor striatal region), whereas those from primarily ventral tegmental area (VTA) project to the NAcc, a ventral striatal region (Morales and Margolis, 2017). The dopamine signal from the SNc to putamen encodes timing and initiation (i.e., if and when) of planned movements (Howe and Dombeck, 2016; Klaus et al., 2019), while dopamine signal from VTA to NAcc encodes the force or vigor of motivated movements (Hughes et al., 2020); Reviewed in (Alm, 2021). In one study, Neef et al (Neef et al., 2018). reported that among the BG areas, only the right NAcc differed in the volumetric comparisons between 33 AWS and controls, suggesting that NAcc function of interfacing cognition, emotion, and action might be affected in speakers who stutter. Though the NAcc has not been a focus of investigation in stuttering to date, it is an area that may be of relevance to stuttering neurophysiology given its role in interfacing limbic and motor areas and is relevant to encoding the motivation to move (Goto and Grace, 2008; Floresco, 2015), that is, it plays a central role in emotional evaluation, reward, and motivation.

The motivational value of movement as encoded by NAcc may have a particular relevance to speech occurring in a goal directed, social setting, as opposed to speech occurring in solo. The situational variability of stuttering, and in particular, the observation of little to no stuttering when speaking to oneself, is of relevance here as it may relate to the difference in dopaminergic activity that affects striatal function and the connectivity to cerebral areas these striatal structures interface during speech in social settings versus speech that is not goal directed. The dopaminergic neurons have also been reported to have greater energy demands (Pacelli et al., 2015; Pissadaki and Bolam, 2013). It has been reported that brain areas with high energy demands coincide with those areas that are significantly different in brain anatomy in stuttering (Chow et al., 2020; Boley et al., 2021) (see review in Alm, (Alm, 2021)) and these undergo rapid growth during early childhood. The high metabolic demands in the dopamine system during dynamic periods of neurodevelopment, combined with possible deficits in connections among circuits that enable learning and execution of automatized motor sequences such as is the case in speech, may be affected in stuttering starting close to stuttering onset.

Kotz and colleagues have argued for the role of additional subcortical

structures, including the basal ganglia (putamen), thalamus, and cerebellum, in temporal processing relevant to speech processing (Kotz and Schwartze, 2010; Kotz et al., 2016). Specifically, the basal ganglia and cerebellum are engaged in detecting and predicting temporal regularities, which is critical during speech acquisition, as they facilitate establishing basic routines that can lead to more complex behavior. Acquiring these routines requires the integration of auditory and sensorimotor information. Animal tracing and unit recording studies have shown that the cerebellum has direct inputs from the cochlear nuclei that enables rapid auditory transmission for temporal processing. The cerebellar dentate outputs to the thalamus, which projects to cortical motor areas that connects to the basal ganglia. This forms a network that links together cerebellar, auditory, and frontal-striatal circuitries, supporting the acquisition of basic motor routines (Akkal et al., 2007; Dum and Strick, 2003).

In the case of stuttering, we speculate that earlier occurring structural deficits in the striatal putamen could negatively affect the acquisition of basic speech routines that are efficiently encoded through their temporal structure. Inefficient acquisition of these speech motor routines could lead to increased demand for constant sensory monitoring and corrective action that involves the cerebellar networks in children who stutter. In the present study, greater WMV around the dentate nucleus into the cerebellar peduncles was observed in both persistent and recovered CWS, but this was particularly greater in rCWS and this pattern increased with age. The greater WMV in this area may indicate a compensatory development of efferent fibers along the cerebellar dentato-thalamocortical loop. This development appears to be insufficient on its own to lead to recovery but may support an important functional increase to compensate for the deficit in the BGTC. These findings highlight the importance of considering the role of temporal processing in the pathophysiology of stuttering.

4.5. Strengths and limitations

To the best of our knowledge, this study involved the largest sample of MRI scans collected from a group of preschool- and school-age CWS and fluent age-matched peers, which allowed us to examine CWS close to the stuttering onset and later childhood when the chance of recovery diminishes. Our longitudinal experimental design allowed us to determine the clinical trajectories of each subject (persistent, recovered, and control). Even though we followed our participants for up to 4 years, it is possible that some of the pCWS included in our study may recover in later childhood or adolescence. However, chances of late recovery should be a minority (Yairi and Ambrose, 1999) and are not expected to significantly alter the present findings.

The results related to rCWS need to be interpreted with caution because the sample size for rCWS was relatively small (N = 23). Due to the small sample size in rCWS, preschool- and school-age children who recovered from stuttering were not analyzed separately as was done in pCWS. Studies employing small sample sizes are more prone to sampling error and at a greater chance of both type I and II errors (Button et al., 2013). The findings related to stuttering recovery therefore will need to be replicated and confirmed in future larger studies.

It is likely that there are several biological, cognitive and environmental factors that influence the anomalous development of gray and white matter in children who stutter. We used sex, IQ and SES as proxies to controls for the potential effects of these factors. However, it is impossible to control for all the potential effects such as handedness and speech-language measures in our statistical models. These effects warrant further analyses in the future, in light of previous studies that have linked behavioral and demographic factors as potential predictors of stuttering persistence, such as speech sound accuracy, expressive/receptive language scores, and stuttering frequency (Singer et al., 2020, 2022), the level of performance on nonword repetition (Spencer and Weber-Fox, 2014), time since onset (Yairi and Ambrose, 1999), and family history of persistent stuttering (Singer et al., 2020; Walsh et al., 2018).

5. Conclusion

Regional gray and white matter volume differences across the whole brain were examined in preschool- and school-age CWS (both persistent and recovered) compared to age matched peers in the largest MRI dataset collected for this clinical population to date. Longitudinally collected scans that spanned up to 4 years per participant allowed tracking of developmental trajectories that differentiated among the groups. The results provide broad support for a possible BGTC network deficit starting at the early phase (preschool-age) of the disorder, involving the putamen, nucleus accumbens, left IFG/vPMC, and corticostriatal tracts. The deficits in input regions of the BGTC network appear to affect the output regions of the network including the thalamus in later phases of stuttering (school-age). The current data also provide insights into neural bases of natural recovery from stuttering during childhood. Children who recover from stuttering showed increased WMV in motor projection fibers, left AF, corpus callosum, and cerebellar peduncle around the dentate nuclei, suggesting that normalization or successful compensation of stuttering-linked neural deficits. Similar volume increases in corpus callosum, and cerebellar peduncle were also observed in pCWS, indicating an incomplete compensation. These results provide substantial new insights into possible neural bases of stuttering onset, persistence, and recovery during childhood.

Declaration of Competing Interest

The authors declare that they have no known competing financial interests or personal relationships that could have appeared to influence the work reported in this paper.

Data Availability

Data will be made available on request.

Appendix A. Supporting information

Supplementary data associated with this article can be found in the online version at doi:10.1016/j.dcn.2023.101224.

References

Akkal, D., Dum, R.P., Strick, P.L., 2007. Supplementary motor area and presupplementary motor area: targets of basal ganglia and cerebellar output. J. Neurosci. 27 (40), 10659–10673. https://doi.org/10.1523/JNEUROSCI.3134-07.2007.

Alm, P.A., 2004. Stuttering and the basal ganglia circuits: a critical review of possible relations. J. Commun. Disord. 37 (4), 325–369. https://doi.org/10.1016/j.jcomdis.2004.03.001.

Alm, P.A., 2021. The dopamine system and automatization of movement sequences: a review with relevance for speech and stuttering. Accessed December 24 Front. Hum. Neurosci. 15. https://doi.org/10.3389/fnhum.2021.661880.

Almli, C.R., Rivkin, M.J., McKinstry, R.C., 2007. The NIH MRI study of normal brain development (Objective-2): newborns, infants, toddlers, and preschoolers. NeuroImage 35 (1), 308–325. https://doi.org/10.1016/j.neuroimage.2006.08.058.

Ashburner, J., 2007. A fast diffeomorphic image registration algorithm. NeuroImage 38 (1), 95–113. https://doi.org/10.1016/j.neuroimage.2007.07.007.

Beal, D.S., Gracco, V.L., Brettschneider, J., Kroll, R.M., De Nil, L.F., 2013. A voxel-based morphometry (VBM) analysis of regional grey and white matter volume abnormalities within the speech production network of children who stutter. Cortex 49 (8), 2151–2161. https://doi.org/10.1016/j.cortex.2012.08.013.

Belyk, M., Kraft, S.J., Brown, S., 2015. Stuttering as a trait or state - an ALE meta-analysis of neuroimaging studies. Eur. J. Neurosci. 41 (2), 275–284. https://doi.org/10.1111/ejn.12765.

Bloodstein, O., Ratner, N.B., 2008. A handbook on stuttering. Thomson Delmar Learn. Accessed March 11, 2022 ⟨http://books.google.com/books?id=aZUhAQAAMAAJ⟩.

Boley, N., Patil, S., Garnett, E.O., et al., 2021. Association between gray matter volume variations and energy utilization in the brain: implications for developmental stuttering. J. Speech Lang. Hear Res. Publ. Online March 9, 1–8. https://doi.org/10.1044/2020_JSLHR-20-00325.

Bostan, A.C., Strick, P.L., 2018. The basal ganglia and the cerebellum: nodes in an integrated network. Nat. Rev. Neurosci. 19 (6), 338–350. https://doi.org/10.1038/s41583-018-0002-7.

Budde, K., 2014. Stuttering, induced fluency, and natural fluency: a hierarchical series of activation likelihood estimation meta-analysis. Brain Lang. 139, 99–107. https://doi.org/10.1016/j.bandl.2014.10.002.

Button, K.S., Ioannidis, J.P.A., Mokrysz, C., et al., 2013. Power failure: why small sample size undermines the reliability of neuroscience. Nat. Rev. Neurosci. 14 (5), 365–376. https://doi.org/10.1038/nrn3475.

Catani, M., Jones, D.K., ffytche, D.H., 2005. Perisylvian language networks of the human brain. Ann. Neurol. 57 (1), 8–16. https://doi.org/10.1002/ana.20319.

Chang, S.E., Guenther, F.H., 2020. Involvement of the cortico-basal ganglia-thalamocortical loop in developmental stuttering. Front Psychol. 10, 3088. https://doi.org/10.3389/fpsyg.2019.03088.

Chang, S.E., Zhu, D.C., 2013. Neural network connectivity differences in children who stutter. Brain 136 (12), 3709–3726. https://doi.org/10.1093/brain/awt275.

Chang, S.E., Erickson, K.I., Ambrose, N.G., Hasegawa-Johnson, M.A., Ludlow, C.L., 2008. Brain anatomy differences in childhood stuttering. NeuroImage 39 (3), 1333–1344. https://doi.org/10.1016/j.neuroimage.2007.09.067.

Chang, S.E., Zhu, D.C., Choo, A.L., Angstadt, M., 2015. White matter neuroanatomical differences in young children who stutter. Brain 138 (Pt 3), 694–711. https://doi.org/10.1093/brain/awu400.

Chang, S.E., Chow, H.M., Wieland, E.A., McAuley, J.D., 2016. Relation between functional connectivity and rhythm discrimination in children who do and do not stutter. NeuroImage: Clin. 12, 442–450. https://doi.org/10.1016/j.nicl.2016.08.021.

Chang, S.E., Angstadt, M., Chow, H.M., et al., 2018. Anomalous network architecture of the resting brain in children who stutter. J. Fluen. Disord. 55, 46–67. https://doi.org/10.1016/j.jfludis.2017.01.002.

Chang, S.E., Garnett, E.O., Etchell, A., Chow, H.M., 2019. Functional and neuroanatomical bases of developmental stuttering: current insights. Neuroscientist 25 (6), 566–582. https://doi.org/10.1177/1073858418803594.

Chen, C.H., Fremont, R., Arteaga-Bracho, E.E., Khodakhah, K., 2014. Short latency cerebellar modulation of the basal ganglia. Nat. Neurosci. 17 (12), 1767–1775. https://doi.org/10.1038/nn.3868.

Choo, A.L., Chang, S.E., Zengin-Bolatkale, H., Ambrose, N.G., Loucks, T.M., 2012. Corpus callosum morphology in children who stutter. J. Commun. Disord. 45 (4), 279–289. https://doi.org/10.1016/j.jcomdis.2012.03.004.

Chow, H.M., Chang, S.E., 2017. White matter developmental trajectories associated with persistence and recovery of childhood stuttering: white matter development in children who stutter. Hum. Brain Mapp. Publ. Online. https://doi.org/10.1002/hbm.23590.

Chow, H.M., Garnett, E.O., Li, H., et al., 2020. Linking lysosomal enzyme targeting genes and energy metabolism with altered gray matter volume in children with persistent stuttering. Neurobiol. Lang. 1 (3), 365–380. https://doi.org/10.1162/nol_a_00017.

Civier, O., Kronfeld-Duenias, V., Amir, O., Ezrati-Vinacour, R., Ben-Shachar, M., 2015. Reduced fractional anisotropy in the anterior corpus callosum is associated with reduced speech fluency in persistent developmental stuttering. Brain Lang. 143, 20–31. https://doi.org/10.1016/j.bandl.2015.01.012.

Connally, E.L., Ward, D., Howell, P., Watkins, K.E., 2014. Disrupted white matter in language and motor tracts in developmental stuttering. Brain Lang. 131, 25–35. https://doi.org/10.1016/j.bandl.2013.05.013.

Cox, R.W., Chen, G., Glen, D.R., Reynolds, R.C., Taylor, P.A., 2017. FMRI clustering in AFNI: false-positive rates redux. Brain Connect. 7 (3), 152–171. https://doi.org/10.1089/brain.2016.0475.

Dick, A.S., Garic, D., Graziano, P., Tremblay, P., 2019. The frontal aslant tract (FAT) and its role in speech, language and executive function. Cortex 111, 148–163. https://doi.org/10.1016/j.cortex.2018.10.015.

Dum, R.P., Strick, P.L., 2003. An unfolded map of the cerebellar dentate nucleus and its projections to the cerebral cortex. J. Neurophysiol. 89 (1), 634–639. https://doi.org/10.1152/jn.00626.2002.

Floresco, S.B., 2015. The nucleus accumbens: an interface between cognition, emotion, and action. Annu Rev. Psychol. 66, 25–52. https://doi.org/10.1146/annurev-psych-010213-115159.

Foundas, A.L., Cindass, R., Mock, J.R., Corey, D.M., 2013. Atypical caudate anatomy in children who stutter. Percept. Mot. Skills 116 (2), 528–543. https://doi.org/10.2466/15.10.PMS.116.2.528-543.

Friederici, A.D., 2006. The neural basis of language development and its impairment. Neuron 52 (6), 941–952. https://doi.org/10.1016/j.neuron.2006.12.002.

Garnett, E.O., Chow, H.M., Nieto-Castañón, A., Tourville, J.A., Guenther, F.H., Chang, S.E., 2018. Anomalous morphology in left hemisphere motor and premotor cortex of children who stutter. Brain 141 (9), 2670–2684. https://doi.org/10.1093/brain/awy199.

Gilmore, J.H., Knickmeyer, R.C., Gao, W., 2018. Imaging structural and functional brain development in early childhood. Nat. Rev. Neurosci. 19 (3), 123–137. https://doi.org/10.1038/nrn.2018.1.

Goerendt, I.K., Messa, C., Lawrence, A.D., Grasby, P.M., Piccini, P., Brooks, D.J., 2003. Dopamine release during sequential finger movements in health and Parkinson's disease: a PET study. Brain 126 (2), 312–325. https://doi.org/10.1093/brain/awg035.

Gogtay, N., Thompson, P.M., 2010. Mapping gray matter development: implications for typical development and vulnerability to psychopathology. Brain Cogn. 72 (1), 6–15. https://doi.org/10.1016/j.bandc.2009.08.009.

Gogtay, N., Giedd, J.N., Lusk, L., et al., 2004. Dynamic mapping of human cortical development during childhood through early adulthood. Proc. Natl. Acad. Sci. 101 (21), 8174–8179. https://doi.org/10.1073/pnas.0402680101.

Goto, Y., Grace, A.A., 2008. Limbic and cortical information processing in the nucleus accumbens. Trends Neurosci. 31 (11), 552–558. https://doi.org/10.1016/j.tins.2008.08.002.

Guenther, F.H., 2006. Cortical interactions underlying the production of speech sounds. J. Commun. Disord. 39 (5), 350–365. https://doi.org/10.1016/j.jcomdis.2006.06.013.

Guenther, F.H., 2016. Neural Control of Speech. MIT Press.

Guillaume, B., Hua, X., Thompson, P.M., Waldorp, L., Nichols, T.E., 2014. Fast and accurate modelling of longitudinal and repeated measures neuroimaging data. NeuroImage 94, 287–302. https://doi.org/10.1016/j.neuroimage.2014.03.029.

Hickok, G., 2012. Computational neuroanatomy of speech production. Nat. Rev. Neurosci. 13 (2), 135–145. https://doi.org/10.1038/nrn3158.

Hollingshead A. Four-factor index of social status. Published online 1975.

Howe, M.W., Dombeck, D.A., 2016. Rapid signalling in distinct dopaminergic axons during locomotion and reward. Nature 535 (7613), 505–510. https://doi.org/10.1038/nature18942.

Hughes, R.N., Bakhurin, K.I., Petter, E.A., et al., 2020. Ventral tegmental dopamine neurons control the impulse vector during motivated behavior. Curr. Biol. 30 (14), 2681–2694. https://doi.org/10.1016/j.cub.2020.05.003.

Ibrahim, J.G., Molenberghs, G., 2009. Missing data methods in longitudinal studies: a review. TEST 18 (1), 1–43. https://doi.org/10.1007/s11749-009-0138-x.

Ingham, R.J., Finn, P., Bothe, A.K., 2005. "Roadblocks" revisited: Neural change, stuttering treatment, and recovery from stuttering. J. Fluen. Disord. 30 (2), 91–107. https://doi.org/10.1016/j.jfludis.2005.01.004.

Johnson, C., Liu, Y., Waller, N., Chang, S.E., 2022. Tract profiles of the cerebellar peduncles in children who stutter. Brain Struct. Funct. Publ. Online. https://doi.org/10.1007/s00429-022-02471-4.

Kell, C.A., Neumann, K., von Kriegstein, K., et al., 2009. How the brain repairs stuttering. Brain 132 (Pt 10), 2747–2760. https://doi.org/10.1093/brain/awp185.

Klaus, A., Alves da Silva, J., Costa, R.M., 2019. What, if, and when to move: basal ganglia circuits and self-paced action initiation. Annu. Rev. Neurosci. 42 (1), 459–483. https://doi.org/10.1146/annurev-neuro-072116-031033.

Koenraads, S.P.C., El Marroun, H., Muetzel, R.L., et al., 2019. Stuttering and gray matter morphometry: a population-based neuroimaging study in young children. Brain Lang. 194, 121–131. https://doi.org/10.1016/j.bandl.2019.04.008.

Kotz, S.A., Schwartze, M., 2010. Cortical speech processing unplugged: a timely subcortico-cortical framework. Trends Cogn. Sci. 14 (9), 392–399. https://doi.org/10.1016/j.tics.2010.06.005.

Kotz, S.A., Schwartze, M., Schmidt-Kassow, M., 2009. Non-motor basal ganglia functions: a review and proposal for a model of sensory predictability in auditory language perception. Cortex 45 (8), 982–990. https://doi.org/10.1016/j.cortex.2009.02.010.

Kotz, S.A., Brown, R.M., Schwartze, M., 2016. Cortico-striatal circuits and the timing of action and perception. Curr. Opin. Behav. Sci. 8, 42–45. https://doi.org/10.1016/j.cobeha.2016.01.010.

Kronfeld-Duenias, V., Amir, O., Ezrati-Vinacour, R., Civier, O., Ben-Shachar, M., 2016. The frontal aslant tract underlies speech fluency in persistent developmental stuttering. Brain Struct. Funct. 221 (1), 365–381. https://doi.org/10.1007/s00429-014-0912-8.

Lu, C., Peng, D., Chen, C., et al., 2010. Altered effective connectivity and anomalous anatomy in the basal ganglia-thalamocortical circuit of stuttering speakers. Cortex 46 (1), 49–67. https://doi.org/10.1016/j.cortex.2009.02.017.

Maguire, G.A., Riley, G.D., Yu, B.P., 2002. A neurological basis of stuttering? Lancet Neurol. 1 (7), 407. https://doi.org/10.1016/S1474-4422(02)00217-X.

Mills, K.L., Goddings, A.L., Herting, M.M., et al., 2016. Structural brain development between childhood and adulthood: convergence across four longitudinal samples. NeuroImage 141, 273–281. https://doi.org/10.1016/j.neuroimage.2016.07.044.

Montag, C., Bleek, B., Reuter, M., et al., 2019. Ventral striatum and stuttering: Robust evidence from a case-control study applying DARTEL. NeuroImage: Clin. 23, 101890 https://doi.org/10.1016/j.nicl.2019.101890.

Morales, M., Margolis, E.B., 2017. Ventral tegmental area: cellular heterogeneity, connectivity and behaviour. Nat. Rev. Neurosci. 18 (2), 73–85. https://doi.org/10.1038/nrn.2016.165.

Neef, N.E., Anwander, A., Friederici, A.D., 2015. The neurobiological grounding of persistent stuttering: from structure to function. Curr. Neurol. Neurosci. Rep. 15 (9) https://doi.org/10.1007/s11910-015-0579-4.

Neef, N.E., Bütfering, C., Auer, T., et al., 2018. Altered morphology of the nucleus accumbens in persistent developmental stuttering. J. Fluen. Disord. 55, 84–93. https://doi.org/10.1016/j.jfludis.2017.04.002.

Neef, N.E., Angstadt, M., Koenraads, S.P.C., Chang, S.E., 2022. Dissecting structural connectivity of the left and right inferior frontal cortex in children who stutter. Cereb. Cortex. Publ. Online Sept. 4, bhac328. https://doi.org/10.1093/cercor/bhac328.

Oldfield, R.C., 1971. The assessment and analysis of handedness: the Edinburgh inventory. Neuropsychologia 9 (1), 97–113. https://doi.org/10.1016/0028-3932(71)90067-4.

Pacelli, C., Giguère, N., Bourque, M.J., Lévesque, M., Slack, R.S., Trudeau, L.É., 2015. Elevated mitochondrial bioenergetics and axonal arborization size are key contributors to the vulnerability of dopamine neurons. Curr. Biol. 25 (18), 2349–2360. https://doi.org/10.1016/j.cub.2015.07.050.

Packman, A., Onslow, M., Lagopoulos, J., et al., 2022. White matter connectivity in neonates at risk of stuttering: preliminary data. Neurosci. Lett. 781, 136655 https://doi.org/10.1016/j.neulet.2022.136655.

Petacchi, A., Laird, A.R., Fox, P.T., Bower, J.M., 2005. Cerebellum and auditory function: an ALE meta-analysis of functional neuroimaging studies. Hum. Brain Mapp. 25 (1), 118–128. https://doi.org/10.1002/hbm.20137.

Pissadaki, E.K., Bolam, J.P., 2013. The energy cost of action potential propagation in dopamine neurons: clues to susceptibility in Parkinson's disease. Front Comput. Neurosci. 7, 13. https://doi.org/10.3389/fncom.2013.00013.

Reilly, S., Onslow, M., Packman, A., et al., 2013. Natural history of stuttering to 4 years of age: a prospective community-based study. Pediatrics 132 (3), 460–467. https://doi.org/10.1542/peds.2012-3067.

Riley G. SSI-4: Stuttering Severity Instrument - Fourth Edition. PRO-ED; 2009.

Shepherd, G.M.G., 2013. Corticostriatal connectivity and its role in disease. Nat. Rev. Neurosci. 14 (4), 278–291. https://doi.org/10.1038/nrn3469.

Singer, C.M., Hessling, A., Kelly, E.M., Singer, L., Jones, R.M., 2020. Clinical characteristics associated with stuttering persistence: a meta-analysis. J. Speech Lang. Hear Res 63 (9), 2995–3018. https://doi.org/10.1044/2020_JSLHR-20-00096.

Singer, C.M., Otieno, S., Chang, S.E., Jones, R.M., 2022. Predicting persistent developmental stuttering using a cumulative risk approach. J. Speech Lang. Hear Res 65 (1), 70–95. https://doi.org/10.1044/2021_JSLHR-21-00162.

Smith, A., Weber, C., 2017. How stuttering develops: the multifactorial dynamic pathways theory. J. Speech Lang. Hear. Res. 60 (9), 2483. https://doi.org/10.1044/2017_JSLHR-S-16-0343.

Sommer, M., Koch, M.A., Paulus, W., Weiller, C., Büchel, C., 2002. Disconnection of speech-relevant brain areas in persistent developmental stuttering. Lancet 360 (9330), 380–383. https://doi.org/10.1016/S0140-6736(02)09610-1.

Sowell, E.R., Peterson, B.S., Thompson, P.M., Welcome, S.E., Henkenius, A.L., Toga, A. W., 2003. Mapping cortical change across the human life span. Nat. Neurosci. 6 (3), 309–315. https://doi.org/10.1038/nn1008.

Spencer, C., Weber-Fox, C., 2014. Preschool speech articulation and nonword repetition abilities may help predict eventual recovery or persistence of stuttering. J. Fluen. Disord. 41, 32–46. https://doi.org/10.1016/j.jfludis.2014.06.001.

Tamnes, C.K., Herting, M.M., Goddings, A.L., et al., 2017. Development of the cerebral cortex across adolescence: a multisample study of inter-related longitudinal changes in cortical volume, surface area, and thickness. J. Neurosci. 37 (12), 3402–3412. https://doi.org/10.1523/JNEUROSCI.3302-16.2017.

Tremblay, P.L., Bedard, M.A., Langlois, D., Blanchet, P.J., Lemay, M., Parent, M., 2010. Movement chunking during sequence learning is a dopamine-dependant process: a study conducted in Parkinson's disease. Exp. Brain Res. 205 (3), 375–385. https://doi.org/10.1007/s00221-010-2372-6.

Van Riper, C., 1971. The Nature of Stuttering. Prentice Hall,.

Vernooij, M.W., Ikram, M.A., Tanghe, H.L., et al., 2007. Incidental findings on brain MRI in the general population. N. Engl. J. Med 357 (18), 1821–1828. https://doi.org/10.1056/NEJMoa070972.

Walsh, B., Usler, E., Bostian, A., et al., 2018. What are predictors for persistence in childhood stuttering. Semin Speech Lang. 39 (04), 299–312. https://doi.org/10.1055/s-0038-1667159.

Watkins, K.E., Smith, S.M., Davis, S., Howell, P., 2008. Structural and functional abnormalities of the motor system in developmental stuttering. Brain 131 (Pt 1), 50–59. https://doi.org/10.1093/brain/awm241.

Wechsler, D., 1999. WASI: Wechsler abbreviated scale of intelligence. Psychol. Corp.

Wechsler, D., 2012. WPPSI-IV: Wechsler preschool and primary scale of intelligence. Psychological Corporation, Fourth edition. 4th ed. Pearson.

Wilke, M., 2018. A spline-based regression parameter set for creating customized DARTEL MRI brain templates from infancy to old age. Data Brief. 16, 959–966. https://doi.org/10.1016/j.dib.2017.12.001.

Wu, J.C., Maguire, G., Riley, G., et al., 1997. Increased dopamine activity associated with stuttering. Neuroreport 8 (3), 767–770. https://doi.org/10.1097/00001756-199702100-00037.

Wu, T., Hallett, M., 2013. The cerebellum in Parkinson's disease. Brain 136 (Pt 3), 696–709. https://doi.org/10.1093/brain/aws360.

Yairi, E., Ambrose, N., 2013. Epidemiology of stuttering: 21st century advances. J. Fluen. Disord. 38 (2), 66–87. https://doi.org/10.1016/j.jfludis.2012.11.002.

Yairi, E., Ambrose, N.G., 1999. Early childhood stuttering I: persistency and recovery rates. J. Speech Lang. Hear Res 42 (5), 1097–1112. https://doi.org/10.1044/jslhr.4205.1097.

Yairi, E., Ambrose, N.G., 2005. Early childhood stuttering for clinicians by clinicians. PRO-ED.

Yairi, E., Ambrose, N.G., Paden, E.P., Throneburg, R.N., 1996. Predictive factors of persistence and recovery: pathways of childhood stuttering. J. Commun. Disord. 29 (1), 51–77. https://doi.org/10.1016/0021-9924(95)00051-8.